# Gas-Phase Conformations and N-Glycosidic Bond Stabilities of Sodium Cationized 2′-Deoxyguanosine and Guanosine: Sodium Cations Preferentially Bind to the Guanine Residue

**Y. Zhu[†], L. A. Hamlow[†], C. C. He[†], J. K. Lee[†], J. Gao[‡], G. Berden[‡], J. Oomens[‡], and M. T. Rodgers[†, *]**

[†]*Department of Chemistry, Wayne State University, Detroit, MI, 48202*

[‡]*Radboud University, Institute for Molecules and Materials, FELIX Laboratory, Toernooiveld 7c, 6525ED Nijmegen, The Netherlands*

**Full citation for Gaussian09, reference 80:**

Frisch, M. J.; Trucks, G. W.; Schlegel, H. B.; Scuseria, G. E.; Robb, M. A.; Cheeseman, J. R.; Scalmani, G.; Barone, V.; Mennucci, B.; Petersson, G. A.; Nakatsuji, H.; Caricato, M.; Li, X.; Hratchian, H. P.; Izmaylov,A. F.; Bloino, J.; Zheng, G.; Sonnenberg, J. L.; Hada, M.; Ehara, M.; Toyota, K.; Fukuda, R.; Hasegawa, J.; Ishida, M.; Nakajima, T.; Honda, Y.; Kitao, O.; Nakai, H.; Vreven, T.; Montgomery Jr., J. A.; Peralta, J. E.; Ogliaro, F.; Bearpark, M. J.; Heyd, J.; Brothers, E. N.; Kudin, K. N.; Staroverov, V. N.; Kobayashi, R.; Normand, J.; Raghavachari, K.; Rendell, A. P.; Burant, J. C.; Iyengar, S. S.; Tomasi, J.; Cossi, M.; Rega, N.; Millam, N. J.; Klene, M.; Knox, J. E.; Cross, J. B.; Bakken, V.; Adamo, C.; Jaramillo, J.; Gomperts, R.; Stratmann, R. E.; Yazyev, O.; Austin, A. J.; Cammi, R.; Pomelli, C.; Ochterski, J. W.; Martin, R. L.; Morokuma, K.; Zakrzewski, V. G.; Voth, G. A.; Salvador, P.; Dannenberg, J. J.; Dapprich, S.; Daniels, A. D.; Farkas, Ö.; Foresman, J. B.; Ortiz, J. V.; Cioslowski, J.; Fox, D. J. Gaussian 09, Gaussian, Inc.: Wallingford, CT, USA, 2009.

**Table S1.** Relative Enthalpies and Free Energies of Stable Low-Energy Conformers of $[dGuo+Na]^+$ at 0 and 298 K in kJ/mol[α]

| Species | Conformer | $\Delta H_0$ | $\Delta H_{298}$ | $\Delta G_{298}$ | *P* | Guanine | Sugar Puckering |
|---|---|---|---|---|---|---|---|
| $[dGuo+Na]^+$ | B1(O6N7) | **0.0** | **0.0** | **0.0** | 173.3° | *anti* | C2'-endo ($^2T_3$) |
| | B2(O6N7) | 0.0 | 0.0 | 0.1 | 173.3° | *anti* | C2'-endo ($^2T_3$) |
| | B3(O6N7) | 0.1 | 0.0 | 0.2 | 170.8° | *anti* | C2'-endo ($^2T_3$) |
| | B4(O6N7) | 0.1 | 0.0 | 0.4 | 173.4° | *anti* | C2'-endo ($^2T_3$) |
| | B5(O6N7) | 0.2 | 0.0 | 0.5 | 173.4° | *anti* | C2'-endo ($^2T_3$) |
| | B6(O6N7) | 3.1 | 3.6 | 2.6 | 12.1° | *anti* | C3′-endo ($^3T_2$) |
| | B7(O6N7) | 3.1 | 3.6 | 2.7 | 12.1° | *anti* | C3'-endo ($^3T_2$) |
| | B8(O6N7) | 3.1 | 3.6 | 2.8 | 12.1° | *anti* | C3'-endo ($^3T_2$) |
| | B9(O6N7) | 1.6 | 1.6 | 6.4 | 160.3° | *syn* | C2'-endo ($^2T_1$) |
| | B10(O6N7) | 11.5 | 12.3 | 6.5 | 146.7° | *anti* | C2′-endo ($^2T_1$) |
| | B11(O6N7) | 6.4 | 6.2 | 7.6 | 9.9° | *anti* | C3'-endo ($^3T_2$) |
| | B12(O6N7) | 8.5 | 8.8 | 7.8 | 181.3° | *anti* | C3'-exo ($_3T^2$) |
| | B13(O6N7) | 8.7 | 8.8 | 8.2 | 181.4° | *anti* | C3'-exo ($_3T^2$) |
| | B14(O6N7) | 12.1 | 11.0 | 10.1 | 31.8° | *anti* | C3′-endo ($^3T_4$) |
| | B15(O6N7) | 14.0 | 13.8 | 14.5 | 199.8° | *anti* | C3′-exo ($_3T^4$) |
| | B16(O6N7) | 18.1 | 18.5 | 14.9 | 134.2° | *anti* | C1′-exo ($_1T^2$) |
| | B17(O6N7) | 14.8 | 14.5 | 15.3 | 200.1° | *anti* | C3'-exo ($_3T^4$) |
| | B18(O6N7) | 17.7 | 18.2 | 15.9 | 165.3° | *syn* | C2'-endo ($^2T_3$) |
| | B19(O6N7) | 17.2 | 17.5 | 16.6 | 196.6° | *anti* | C3'-exo ($_3T^2$) |
| | B20(O6N7) | 21.2 | 22.1 | 16.9 | 41.3° | *anti* | C4'-exo ($_4T^3$) |
| | B21(O6N7) | 19.7 | 19.6 | 19.7 | 213.5° | *anti* | C3'-exo ($_3T^4$) |
| | B22(O6N7) | 23.5 | 24.0 | 20.9 | 26.0° | *anti* | C3'-endo ($^3T_4$) |
| | B23(O6N7) | 26.5 | 27.8 | 21.3 | 181.4° | *anti* | C3'-exo ($_3T^2$) |
| | B24(O6N7) | 26.5 | 27.8 | 21.4 | 181.4° | *anti* | C3'-exo ($_3T^2$) |
| | B25(O6N7) | 21.9 | 22.1 | 21.7 | 212.7° | *anti* | C3'-exo ($_3T^4$) |
| | B26(O6N7) | 21.9 | 22.1 | 21.8 | 212.8° | *anti* | C3'-exo ($_3T^4$) |
| | B27(O6N7) | 19.2 | 18.1 | 21.8 | 35.2° | *syn* | C3′-endo ($^3T_4$) |
| | B28(O6N7) | 26.1 | 26.1 | 23.7 | 32.4° | *anti* | C3'-endo ($^3T_4$) |
| | B29(O6N7) | 26.2 | 25.4 | 25.4 | 186.0° | *anti* | C3'-exo ($_3T^2$) |
| | T1(N3O4'O5') | 54.2 | 53.1 | 56.9 | 334.7° | *syn* | C2′-exo ($_2T^1$) |
| | T2(N3O4'O5') | 58.4 | 57.8 | 60.3 | 163.4° | *syn* | C2'-endo ($^2T_3$) |
| | T3(N3O4'O5') | 58.4 | 57.8 | 60.4 | 163.4° | *syn* | C2'-endo ($^2T_3$) |
| | B1(O4'O5') | 104.2 | 103.0 | 106.3 | 188.3° | *syn* | C3′-exo ($_3T^2$) |
| | B1(N3O3') | 129.9 | 129.7 | 131.1 | 138.5° | *anti* | C1′-exo ($_1T^2$) |

[α]Energetics based on single-point energy calculations performed at the B3LYP/6-311+G(2d,2p) level of theory, including ZPE and thermal corrections based on the B3LYP/6-311+G(d,p) optimized structures and vibrational frequencies.

**Table S2.** Relative Enthalpies and Free Energies of Stable Low-Energy Conformers of $[Guo+Na]^+$ at 0 and 298 K in kJ/mol[α]

| Species | Conformer | $\Delta H_0$ | $\Delta H_{298}$ | $\Delta G_{298}$ | *P* | Guanine | Sugar Puckering |
|---|---|---|---|---|---|---|---|
| $[Guo+Na]^+$ | B1(O6N7) | 1.1 | 1.9 | **0.0** | 169.0° | *anti* | C2′-endo ($^2T_3$) |
| | B2(O6N7) | **0.0** | **0.0** | 0.5 | 155.9° | *syn* | C2′-endo ($^2T_1$) |
| | B3(O6N7) | 3.7 | 4.4 | 3.3 | 14.4° | *anti* | C3′-endo ($^3T_2$) |
| | B4(O6N7) | 7.6 | 8.1 | 6.3 | 173.5° | *anti* | C2'-endo ($^2T_3$) |
| | B5(O6N7) | 6.7 | 7.5 | 6.9 | 11.9° | *anti* | C3'-endo ($^3T_2$) |
| | B6(O6N7) | 11.5 | 13.0 | 7.0 | 131.5° | *anti* | C1′-exo ($_1T^2$) |
| | B7(O6N7) | 11.5 | 13.0 | 7.1 | 131.5° | *anti* | C1'-exo ($_1T^2$) |
| | B8(O6N7) | 11.3 | 10.8 | 8.7 | 41.1° | *anti* | C4'-exo ($_4T^3$) |
| | B9(O6N7) | 10.0 | 11.0 | 9.0 | 177.0° | *anti* | C2'-endo ($^2T_3$) |
| | B10(O6N7) | 10.1 | 11.0 | 9.1 | 177.0° | *anti* | C2'-endo ($^2T_3$) |
| | B11(O6N7) | 11.0 | 10.8 | 11.0 | 44.4° | *syn* | C4′-exo ($_4T^3$) |
| | B12(O6N7) | 17.4 | 19.0 | 12.7 | 134.1° | *anti* | C1'-exo ($_1T^2$) |
| | B13(O6N7) | 19.3 | 21.1 | 13.7 | 131.8° | *anti* | C1'-exo ($_1T^2$) |
| | B14(O6N7) | 20.0 | 21.7 | 13.9 | 162.3° | *anti* | C2'-endo ($^2T_3$) |
| | B15(O6N7) | 22.7 | 24.1 | 18.1 | 43.0° | *anti* | C4'-exo ($_4T^3$) |
| | B16(O6N7) | 23.3 | 25.1 | 18.3 | 143.2° | *syn* | C1'-exo ($_1T^2$) |
| | B17(O6N7) | 22.5 | 22.7 | 18.8 | 143.5° | *syn* | C1'-exo ($_1T^2$) |
| | B18(O6N7) | 23.6 | 25.0 | 19.0 | 145.3° | *syn* | C2'-endo ($^2T_1$) |
| | B19(O6N7) | 24.5 | 26.3 | 19.2 | 45.0° | *anti* | C4'-exo ($_4T^3$) |
| | B20(O6N7) | 20.6 | 21.5 | 19.4 | 190.0° | *anti* | C3′-exo ($_3T^2$) |
| | B21(O6N7) | 23.1 | 24.1 | 19.9 | 151.7° | *anti* | C2'-endo ($^2T_1$) |
| | B22(O6N7) | 23.1 | 24.1 | 20.0 | 151.8° | *anti* | C2'-endo ($^2T_1$) |
| | B23(O6N7) | 22.9 | 24.1 | 20.2 | 168.7° | *syn* | C2'-endo ($^2T_3$) |
| | B24(O6N7) | 24.9 | 25.9 | 21.9 | 158.8° | *anti* | C2'-endo ($^2T_1$) |
| | B25(O6N7) | 27.7 | 28.8 | 23.6 | 36.5° | *anti* | C4′-exo ($_4T^3$) |
| | B26(O6N7) | 28.5 | 30.2 | 24.7 | 149.0° | *syn* | C2'-endo ($^2T_1$) |
| | B27(O6N7) | 23.4 | 23.3 | 25.1 | 176.7° | *anti* | C2'-endo ($^2T_3$) |
| | T1(N3O4'O5') | 75.2 | 75.0 | 77.4 | 10.0° | *syn* | C3′-endo ($^3T_2$) |
| | T2(N3O4'O5') | 75.2 | 75.1 | 77.5 | 9.9° | *syn* | C3'-endo ($^3T_2$) |
| | B1(N3O2') | 84.2 | 84.0 | 82.7 | 174.6° | *anti* | C2′-endo ($^2T_3$) |
| | B2(N3O2') | 84.2 | 84.0 | 82.8 | 174.6° | *anti* | C2'-endo ($^2T_3$) |
| | T1(N3NH$_2$O2') | 84.6 | 84.3 | 83.5 | 72.9° | *anti* | O4′-endo ($^OT_4$) |
| | T2(N3NH$_2$O2') | 84.9 | 84.4 | 84.0 | 201.8° | *anti* | C3'-exo ($_3T^4$) |
| | T3(N3NH$_2$O2') | 87.9 | 88.1 | 84.7 | 84.2° | *anti* | O4'-endo ($^OT_4$) |
| | B1(N3O4') | 98.5 | 99.2 | 96.8 | 189.2° | *syn* | C3′-exo ($_3T^2$) |
| | B1(O2'O3') | 118.2 | 119.1 | 115.2 | 164.7° | *syn* | C2′-endo ($^2T_3$) |
| | B1(O3'O4') | 120.0 | 119.9 | 121.4 | 213.6° | *anti* | C3′-exo ($_3T^4$) |

[α]Energetics based on single-point energy calculations performed at the B3LYP/6-311+G(2d,2p) level of theory, including ZPE and thermal corrections based on the B3LYP/6-311+G(d,p) optimized structures and vibrational frequencies.

**Table S3.** Relative Enthalpies and Free Energies of Stable Low-Energy Tautomeric Conformers of $[dGuo+Na]^+$ and $[Guo+Na]^+$ at 0 and 298 K in kJ/mol[α]

| Species | Conformer | $\Delta H_0$ | $\Delta H_{298}$ | $\Delta G_{298}$ | *P* | Guanine Orientation | Sugar Puckering |
|---|---|---|---|---|---|---|---|
| $[dGuo+Na]^+$ | B1(O6N7)t3 | 29.6 | 29.1 | 32.2 | 155.4° | *syn* | C2'-endo ($^2T_1$) |
| | B1(N1O6)t7 | 38.0 | 37.7 | 38.3 | 7.6° | *anti* | C3'-endo ($^3T_2$) |
| | T1(N3O4'O5')t6 | 44.9 | 43.8 | 46.7 | 156.2° | *syn* | C2'-endo ($^2T_1$) |
| | B1(O6N7)t6 | 51.1 | 51.3 | 50.1 | 170.2° | *anti* | C2'-endo ($^2T_3$) |
| | B1(O6N7)t13 | 50.6 | 49.0 | 53.8 | 150.0° | *syn* | C2'-endo ($^2T_1$) |
| | T1(N3O4'O5')t16 | 117.5 | 116.2 | 119.6 | 113.1° | *syn* | C1'-exo ($_1T^O$) |
| | B1(N1NH)t36 | 131.6 | 130.9 | 131.4 | 177.3° | *anti* | C2′-endo ($^2T_3$) |
| | T1(N3O4'O5')t17 | 132.8 | 131.6 | 134.9 | 351.3° | *syn* | C2'-exo ($_2T^3$) |
| | B1(N1NH)t67 | 137.8 | 137.0 | 138.7 | 7.2° | *anti* | C3'-endo ($^3T_2$) |
| | B1(N1O6)t37 | 141.4 | 141.1 | 139.8 | 173.3° | *anti* | C2'-endo ($^2T_3$) |
| $[Guo+Na]^+$ | B1(O6N7)t3 | 31.1 | 30.3 | 34.2 | 152.7° | *syn* | C2'-endo ($^2T_1$) |
| | B1(N1O6)t7 | 40.6 | 39.7 | 40.8 | 175.7° | *anti* | C2'-endo ($^2T_3$) |
| | T1(N3O4'O5')t6 | 46.1 | 44.8 | 49.0 | 357.2° | *syn* | C2'-exo ($_2T^3$) |
| | B1(O6N7)t6 | 51.9 | 52.2 | 51.2 | 168.6° | *anti* | C2'-endo ($^2T_3$) |
| | B1(O6N7)t13 | 56.1 | 54.8 | 57.5 | 46.1° | *syn* | C4'-exo ($_4T^3$) |
| | B1(N1NH)t36 | 114.7 | 113.5 | 114.6 | 167.1° | *anti* | C2'-endo ($^2T_3$) |
| | T1(N3O4'O5')t16 | 120.2 | 119.1 | 122.1 | 112.4° | *syn* | C1'-exo ($_1T^O$) |
| | B1(N1NH)t37 | 129.9 | 128.7 | 130.4 | 174.2° | *anti* | C2'-endo ($^2T_3$) |
| | B1(N3O2')t17 | 133.8 | 132.2 | 134.8 | 183.0° | *anti* | C3'-exo ($_3T^2$) |
| | B1(N1NH)t67 | 141.1 | 140.1 | 142.1 | 9.8° | *anti* | C3'-endo ($^3T_2$) |

[α]Energetics based on single-point energy calculations performed at the B3LYP/6-311+G(2d,2p) level of theory, including ZPE and thermal corrections based on the B3LYP/6-311+G(d,p) optimized structures and vibrational frequencies.

**Figure Captions**

**Figure S1.** Designations for nucleobase orientation and pseudorotation phase angle, *P* of nucleosides.

**Figure S2.** Stable low-energy conformers of $[dGuo+Na]^+$ involving binding of $Na^+$ to the canonical tautomer of the guanine residue. The $Na^+$ binding modes, orientations of guanine, sugar configurations, and the relative 298 K Gibbs free energies at the B3LYP/6-311+G(2d,2p)//B3LYP/6-311+G(d,p) level of theory are also listed for each structure.

**Figure S3.** Stable low-energy conformers of $[Guo+Na]^+$ involving binding of $Na^+$ to the canonical tautomer of the guanine residue. The $Na^+$ binding modes, orientations of guanine, sugar configurations, and the relative 298 K Gibbs free energies at the B3LYP/6-311+G(2d,2p)//B3LYP/6-311+G(d,p) level of theory are also listed for each structure.

**Figure S4.** Stable conformers of $[dGuo+Na]^+$ involving binding of $Na^+$ to minor tautomers of the guanine residue. Only the most stable mode of binding for each tautomer is shown. The $Na^+$ binding modes, orientations of guanine, sugar configurations, and the relative 298 K Gibbs free energies at the B3LYP/6-311+G(2d,2p)//B3LYP/6-311+G(d,p) level of theory are also listed for each structure.

**Figure S5.** Stable conformers of $[Guo+Na]^+$ involving binding of $Na^+$ to minor tautomers of the guanine residue. Only the most stable mode of binding for each tautomer is shown.The $Na^+$ binding modes, orientations of guanine, sugar configurations, and the relative 298 K Gibbs free energies at the B3LYP/6-311+G(2d,2p)//B3LYP/6-311+G(d,p) level of theory are also listed for each structure.

**Figure S6.** Comparison of the experimental IRMPD action spectrum of $[dGuo+Na]^+$ with the B3LYP/6-311+G(d,p) optimized structures and calculated linear IR spectra for the guanine binding conformers with misalignments shaded in red of $[dGuo+Na]^+$. The B3LYP/6-311+G(2d,2p) relative Gibbs free energies at 298 K, guanine orientation, and sugar puckering are also shown.

**Figure S7.** Comparison of the experimental IRMPD action spectrum of $[dGuo+Na]^+$ with the B3LYP/6-311+G(d,p) optimized structures and calculated linear IR spectrum for the sugar binding conformer with misalignments shaded in red of $[dGuo+Na]^+$. The B3LYP/6-311+G(2d,2p) relative Gibbs free energies at 298 K, guanine orientation, and sugar puckering are also shown.

**Figure S8.** Comparison of the experimental IRMPD action spectrum of $[dGuo+Na]^+$ with the B3LYP/6-311+G(d,p) optimized structures and calculated linear IR spectrum for complexes inovolving binding to minor tautomers of the guanine residue with misalignments shaded in red of $[dGuo+Na]^+$. The B3LYP/6-311+G(2d,2p) relative Gibbs free energies at 298 K, guanine orientation, and sugar puckering are also shown.

**Figure S9.** Comparison of the experimental IRMPD action spectrum of $[Guo+Na]^+$ with the B3LYP/6-311+G(d,p) optimized structures and calculated linear IR spectra for the guanine binding conformers with misalignments shaded in red of $[Guo+Na]^+$. The B3LYP/6-311+G(2d,2p) relative Gibbs free energies at 298 K, guanine orientation, and

sugar puckering are also shown.

**Figure S10.** Comparison of the experimental IRMPD action spectrum of $[Guo+Na]^+$ with the B3LYP/6-311+G(d,p) optimized structures and calculated linear IR spectra for the sugar binding conformers with misalignments shaded in red of $[Guo+Na]^+$. The B3LYP/6-311+G(2d,2p) relative Gibbs free energies at 298 K, guanine orientation, and sugar puckering are also shown.

**Figure S11.** Comparison of the experimental IRMPD action spectrum of $[Guo+Na]^+$ with the B3LYP/6-311+G(d,p) optimized structures and calculated linear IR spectra for complexes involving binding to minor tautomers of the guanine residue with misalignments shaded in red of $[Guo+Na]^+$. The B3LYP/6-311+G(2d,2p) relative Gibbs free energies at 298 K, guanine orientation, and sugar puckering are also shown.

Figure S1.

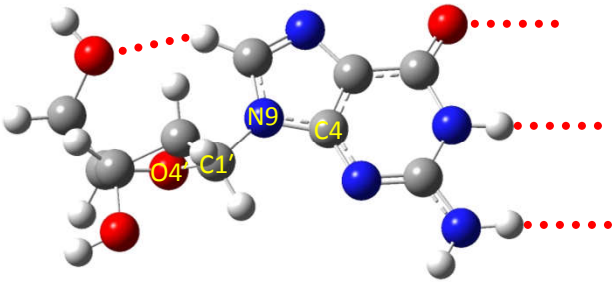


***anti* orientation**

∠C4N9C1′O4′ = 90° to 270°

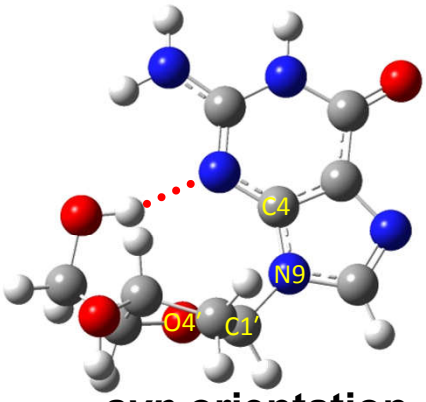


***syn* orientation**

∠C4N9C1′O4′ = –90° to 90°

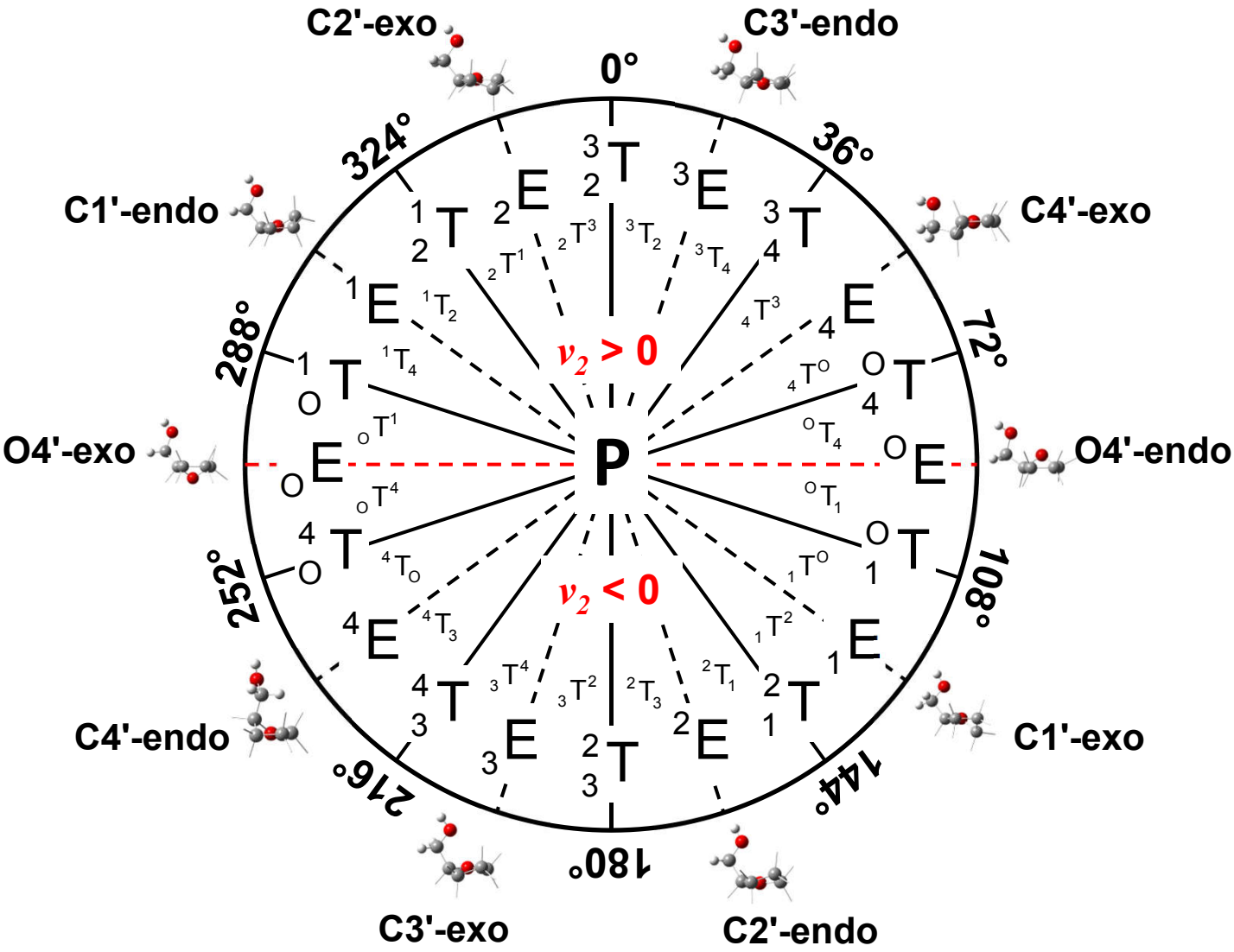

# Figure S2.

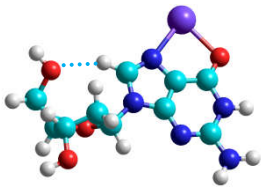

B1(O6N7)
*anti,* C2'-endo ($^2T_3$)
0.0 kJ/mol

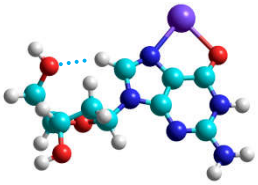

B2(O6N7)
*anti,* C2'-endo ($^2T_3$)
0.1 kJ/mol

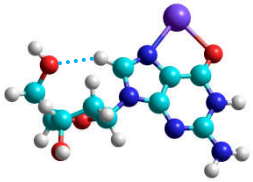

B3(O6N7)
*anti,* C2'-endo ($^2T_3$)
0.2 kJ/mol

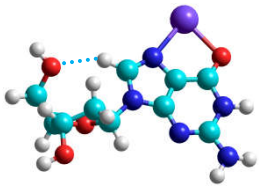

B4(O6N7)
*anti,* C2'-endo ($^2T_3$)
0.4 kJ/mol

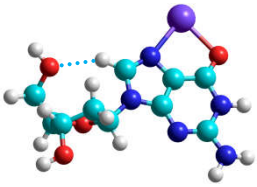

B5(O6N7)
*anti,* C2'-endo ($^2T_3$)
0.5 kJ/mol

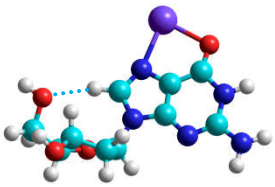

B6(O6N7)
*anti,* C3'-endo ($^3T_2$)
2.6 kJ/mol

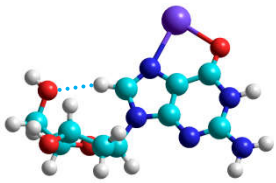

B7(O6N7)
*anti,* C3'-endo ($^3T_2$)
2.7 kJ/mol

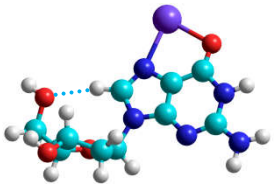

B8(O6N7)
*anti,* C3'-endo ($^3T_2$)
2.8 kJ/mol

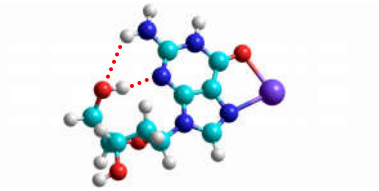

B9(O6N7)
*syn,* C2'-endo ($^2T_1$)
6.4 kJ/mol

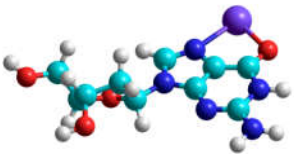

B10(O6N7)
*anti,* C2'-endo ($^2T_1$)
6.5 kJ/mol

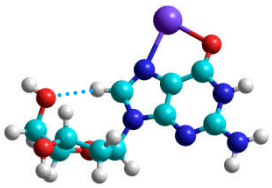

B11(O6N7)
*anti,* C3'-endo ($^3T_2$)
7.6 kJ/mol

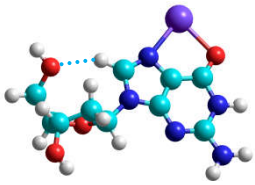

B12(O6N7)
*anti,* C3'-exo ($_3T^2$)
7.8 kJ/mol

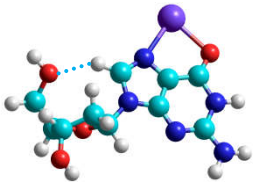

B13(O6N7)
*anti,* C3'-exo ($_3T^2$)
8.2 kJ/mol

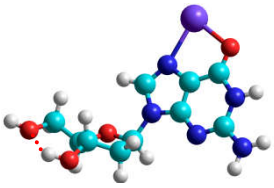

B14(O6N7)
*anti,* C3'-endo ($^3T_4$)
10.1 kJ/mol

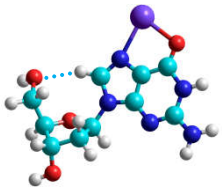

B15(O6N7)
*anti,* C3'-exo ($_3T^4$)
14.5 kJ/mol

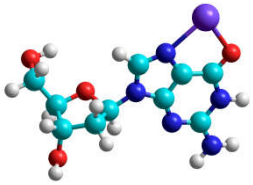

B16(O6N7)
*anti,* C1'-exo ($_1T^2$)
14.9 kJ/mol

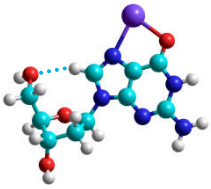

B17(O6N7)
*anti,* C3'-exo ($_3T^4$)
15.3 kJ/mol

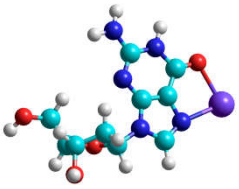

B18(O6N7)
*syn,* C2'-endo ($^2T_3$)
15.9 kJ/mol

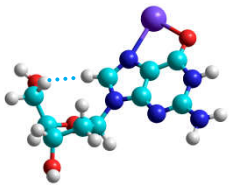

B19(O6N7)
*anti,* C3'-exo ($_3T^2$)
16.6 kJ/mol

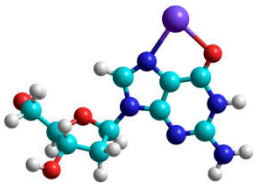

B20(O6N7)
*anti,* C4'-exo ($_4T^3$)
16.9 kJ/mol

$[dGuo+Na]^+$

# Figure S2.

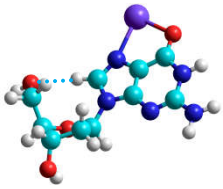

B21(O6N7)
*anti,* C3'-exo ($_3T^4$)
19.7 kJ/mol

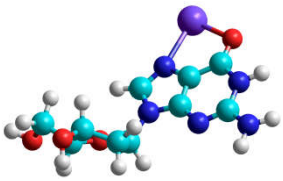

B22(O6N7)
*anti,* C3'-endo ($^3T_4$)
20.9 kJ/mol

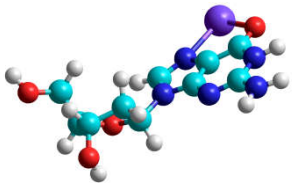

B23(O6N7)
*anti,* C3'-exo ($_3T^2$)
21.3 kJ/mol

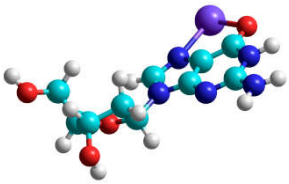

B24(O6N7)
*anti,* C3'-exo ($_3T^2$)
21.4 kJ/mol

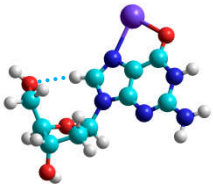

B25(O6N7)
*anti,* C3'-exo ($_3T^4$)
21.7 kJ/mol

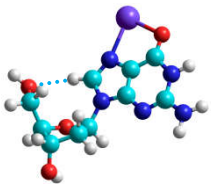

B26(O6N7)
*anti,* C3'-exo ($_3T^4$)
21.8 kJ/mol

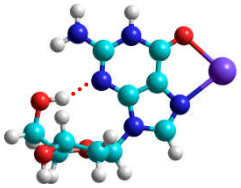

B27(O6N7)
*syn,* C3'-endo ($^3T_4$)
21.8 kJ/mol

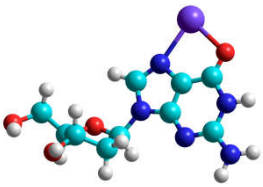

B28(O6N7)
*anti,* C3'-endo ($^3T_4$)
23.7 kJ/mol

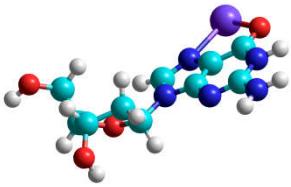

B29(O6N7)
*anti,* C3'-exo ($_3T^2$)
25.4 kJ/mol

T1(N3O4'O5')
*syn,* C2'-exo ($_2T^1$)
56.9 kJ/mol

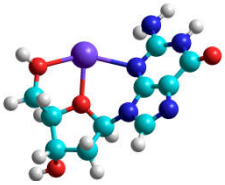

T2(N3O4'O5')
*syn,* C2'-endo ($^2T_3$)
60.3 kJ/mol

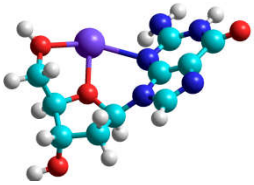

T3(N3O4'O5')
*syn,* C2'-endo ($^2T_3$)
60.4 kJ/mol

B1(O4'O5')
*syn,* C3'-exo ($_3T^2$)
106.3 kJ/mol

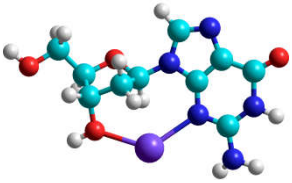

B1(N3O3')
*anti,* C1'-exo ($_1T^2$)
131.1 kJ/mol

[dGuo+Na]$^+$

# Figure S3.

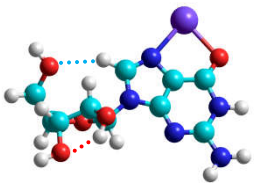

B1(O6N7)
*anti,* C2'-endo ($^2T_3$)
0.0 kJ/mol

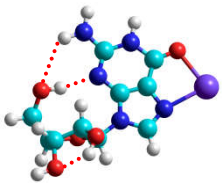

B2(O6N7)
*syn,* C2'-endo ($^2T_1$)
0.5 kJ/mol

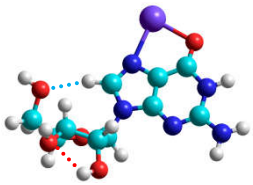

B3(O6N7)
*anti,* C3'-endo ($^3T_2$)
3.3 kJ/mol

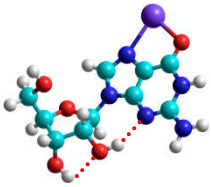

B4(O6N7)
*anti,* C2'-endo ($^2T_3$)
6.3 kJ/mol

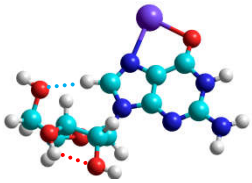

B5(O6N7)
*anti,* C3'-endo ($^3T_2$)
6.9 kJ/mol

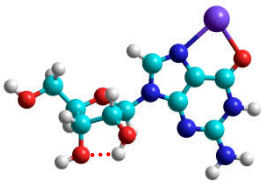

B6(O6N7)
*anti,* C1'-exo ($_1T^2$)
7.0 kJ/mol

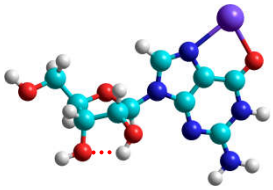

B7(O6N7)
*anti,* C1'-exo ($_1T^2$)
7.1 kJ/mol

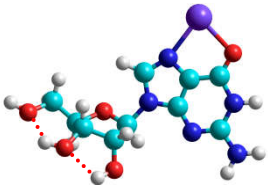

B8(O6N7)
*anti,* C4'-exo ($_4T^3$)
8.7 kJ/mol

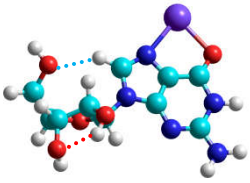

B9(O6N7)
*anti,* C2'-endo ($^2T_3$)
9.0 kJ/mol

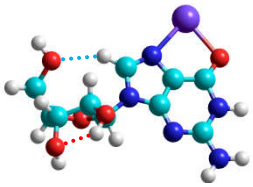

B10(O6N7)
*anti,* C2'-endo ($^2T_3$)
9.1 kJ/mol

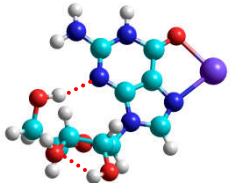

B11(O6N7)
*syn,* C4'-exo ($_4T^3$)
11.0 kJ/mol

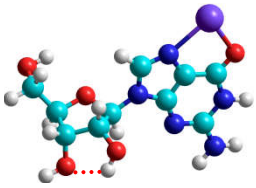

B12(O6N7)
*anti,* C1'-exo ($_1T^2$)
12.7 kJ/mol

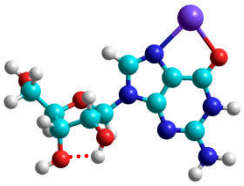

B13(O6N7)
*anti,* C1'-exo ($_1T^2$)
13.7 kJ/mol

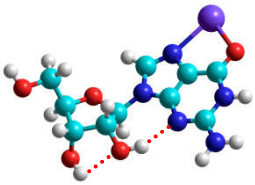

B14(O6N7)
*anti,* C2'-endo ($^2T_3$)
13.9 kJ/mol

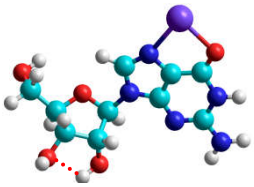

B15(O6N7)
*anti,* C4'-exo ($_4T^3$)
18.1 kJ/mol

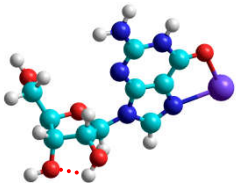

B16(O6N7)
*syn,* C1'-exo ($_1T^2$)
18.3 kJ/mol

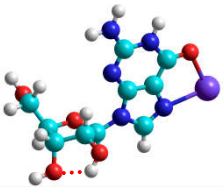

B17(O6N7)
*syn,* C1'-exo ($_1T^2$)
18.8 kJ/mol

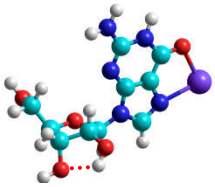

B18(O6N7)
*syn,* C2'-endo ($^2T_1$)
19.0 kJ/mol

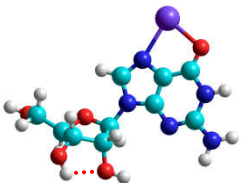

B19(O6N7)
*anti,* C4'-exo ($_4T^3$)
19.2 kJ/mol

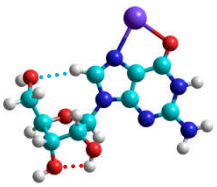

B20(O6N7)
*anti,* C3'-exo ($_3T^2$)
19.4 kJ/mol

$[Guo+Na]^+$

# Figure S3.

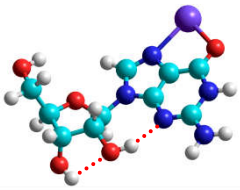

B21(O6N7)
*anti,* C2'-endo ($^2T_1$)
19.9 kJ/mol

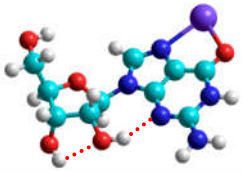

B22(O6N7)
*anti,* C2'-endo ($^2T_1$)
20.0 kJ/mol

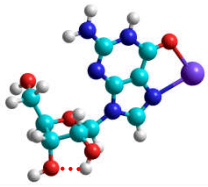

B23(O6N7)
*syn,* C2'-endo ($^2T_3$)
20.2 kJ/mol

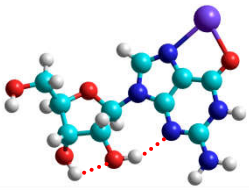

B24(O6N7)
*anti,* C2'-endo ($^2T_1$)
21.9 kJ/mol

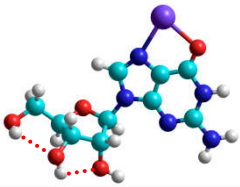

B25(O6N7)
*anti,* C4'-exo ($_4T^3$)
23.6 kJ/mol

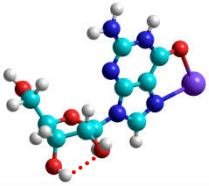

B26(O6N7)
*syn,* C2'-endo ($^2T_1$)
24.7 kJ/mol

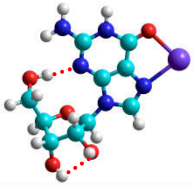

B27(O6N7)
*syn,* C2'-endo ($^2T_3$)
25.1 kJ/mol

T1(N3O4'O5')
*syn,* C3'-endo ($^3T_2$)
77.4 kJ/mol

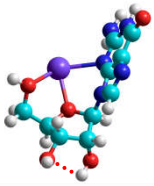

T2(N3O4'O5')
*syn,* C3'-endo ($^3T_2$)
77.5 kJ/mol

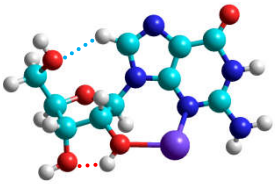

B1(N3O2')
*anti,* C2'-endo ($^2T_3$)
82.7 kJ/mol

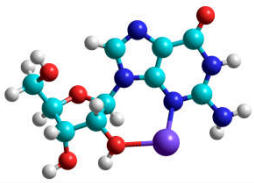

B2(N3O2')
*anti,* C2'-endo ($^2T_3$)
82.8 kJ/mol

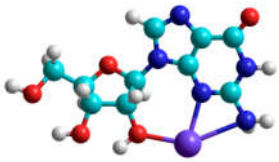

T1(N3NH$_2$O2')
*anti,* O4'-endo ($^OT_4$)
83.5 kJ/mol

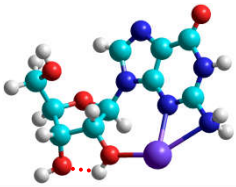

T2(N3NH$_2$O2')
*anti,* C3'-exo ($_3T^4$)
84.0 kJ/mol

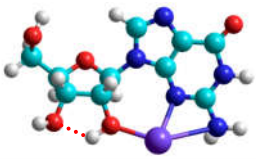

T3(N3NH$_2$O2')
*anti,* O4'-endo ($^OT_4$)
84.7 kJ/mol

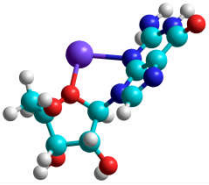

B1(N3O4')
*syn,* C3'-exo ($_3T^2$)
96.8 kJ/mol

B1(O2'O3')
*syn,* C2'-endo ($^2T_3$)
115.2 kJ/mol

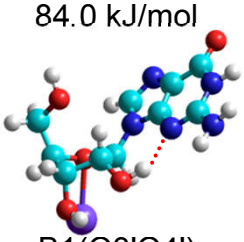

B1(O3'O4')
*anti,* C3'-exo ($_3T^4$)
121.4 kJ/mol

[Guo+Na]$^+$

# Figure S4.

B1(O6N7)t3
*syn,* C2'-endo ($^2T_1$)
32.2 kJ/mol

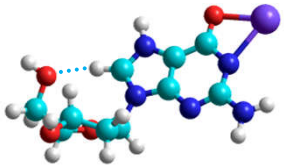

B1(N1O6)t7
*anti,* C3'-endo ($^3T_2$)
38.3 kJ/mol

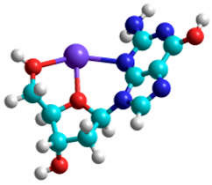

T1(N3O4'O5')t6
*syn,* C2'-endo ($^2T_1$)
46.7 kJ/mol

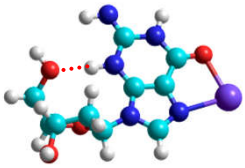

B1(O6N7)t13
*syn,* C2'-endo ($^2T_1$)
53.8 kJ/mol

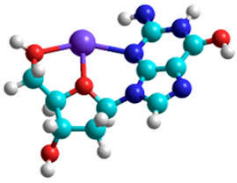

T1(N3O4'O5')t16
*syn,* C1'-exo ($_1T^O$)
119.6 kJ/mol

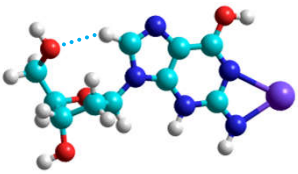

B1(N1NH)t36
*anti,* C2'-endo ($^2T_3$)
131.4 kJ/mol

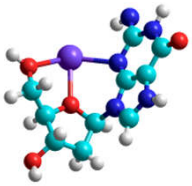

T1(N3O4'O5')t17
*syn,* C2'-exo ($_2T^3$)
134.9 kJ/mol

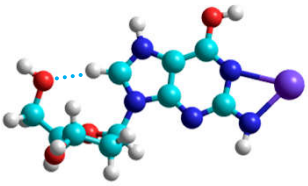

B1(N1NH)t67
*anti,* C3'-endo ($^3T_2$)
138.7 kJ/mol

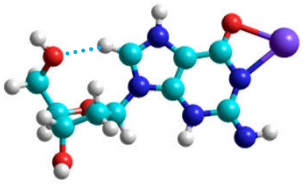

B1(N1O6)t37
*anti,* C2'-endo ($^2T_3$)
139.8 kJ/mol

[dGuo+Na]$^+$

# Figure S5.

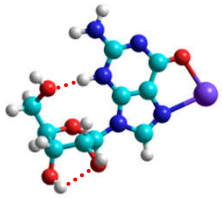

B1(O6N7)t3
*syn,* C2'-endo ($^2T_1$)
34.2 kJ/mol

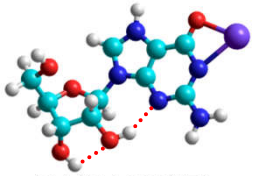

B1(N1O6)t7
*anti,* C2'-endo ($^2T_3$)
40.8 kJ/mol

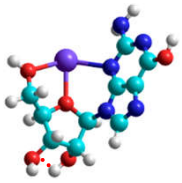

T1(N3O4'O5')t6
*syn,* C2'-exo ($_2T^3$)
49.0 kJ/mol

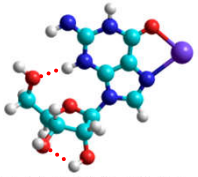

B1(O6N7)t13
*syn,* C4'-exo ($_4T^3$)
57.5 kJ/mol

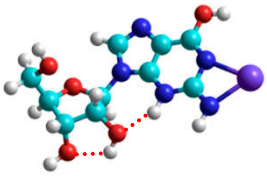

B1(N1NH)t36
*anti,* C2'-endo ($^2T_3$)
114.6 kJ/mol

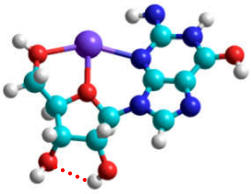

T1(N3O4'O5')t16
*syn,* C1'-exo ($_1T^O$)
122.1 kJ/mol

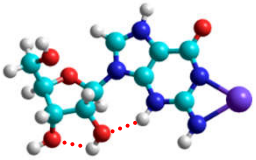

B1(N1NH)t37
*anti,* C2'-endo ($^2T_3$)
130.4 kJ/mol

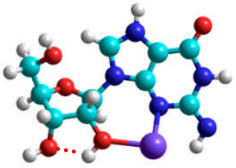

B1(N3O2')t17
*anti,* C3'-exo ($_3T^2$)
134.8 kJ/mol

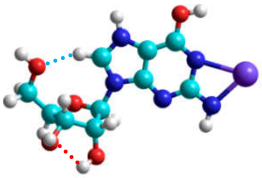

B1(N1NH)t67
*anti,* C3'-endo ($^3T_2$)
142.1 kJ/mol

[Guo+Na]$^+$

Figure S6.

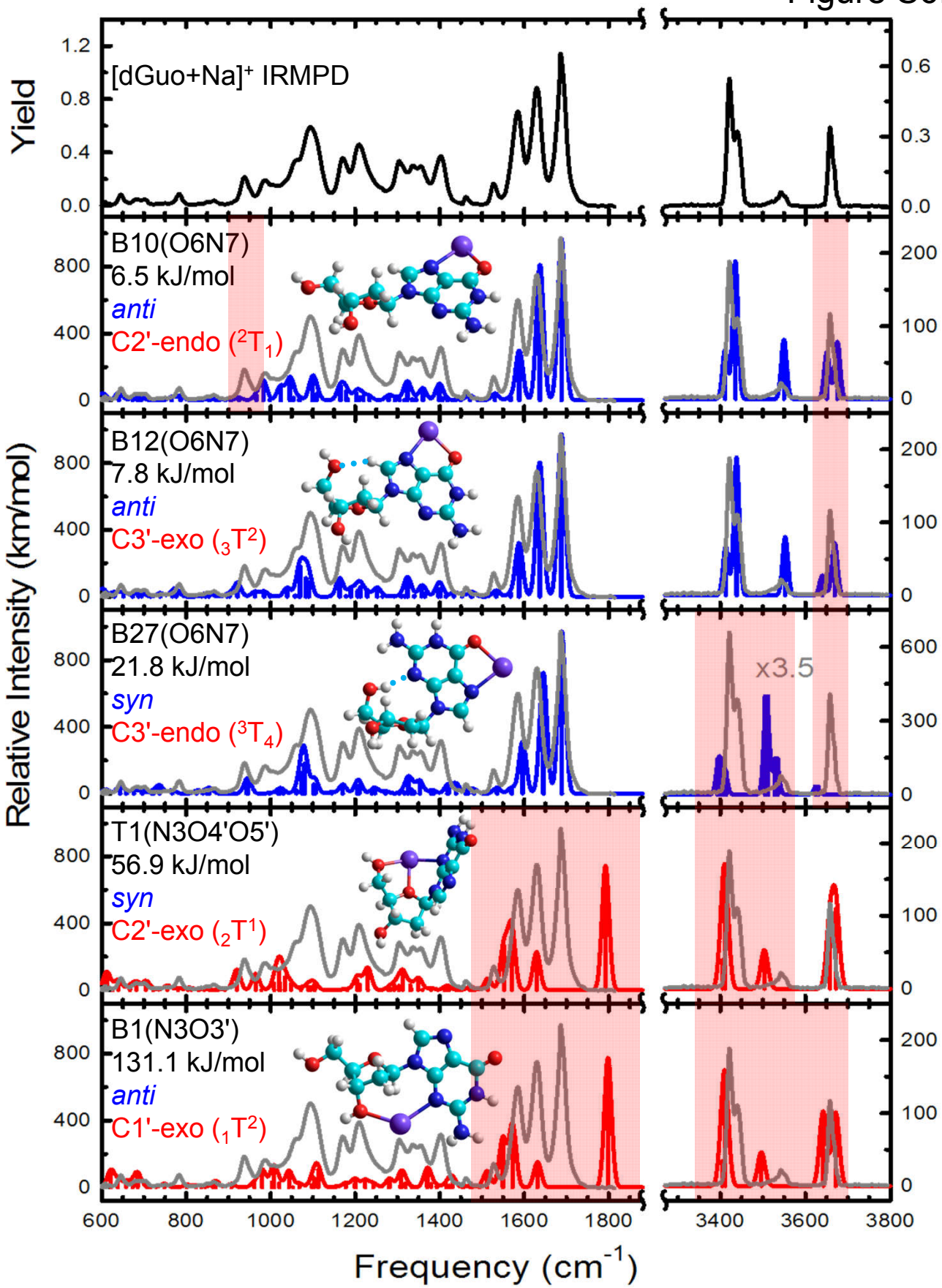
[dGuo+Na]+ IRMPD
Yield
B10(O6N7)
6.5 kJ/mol
anti
C2'-endo (2T1)
B12(O6N7)
7.8 kJ/mol
anti
C3'-exo (3T2)
B27(O6N7)
21.8 kJ/mol
syn
C3'-endo (3T4)
x3.5
T1(N3O4'O5')
56.9 kJ/mol
syn
C2'-exo (2T1)
B1(N3O3')
131.1 kJ/mol
anti
C1'-exo (1T2)
Relative Intensity (km/mol)
Frequency (cm-1)

Figure S7.

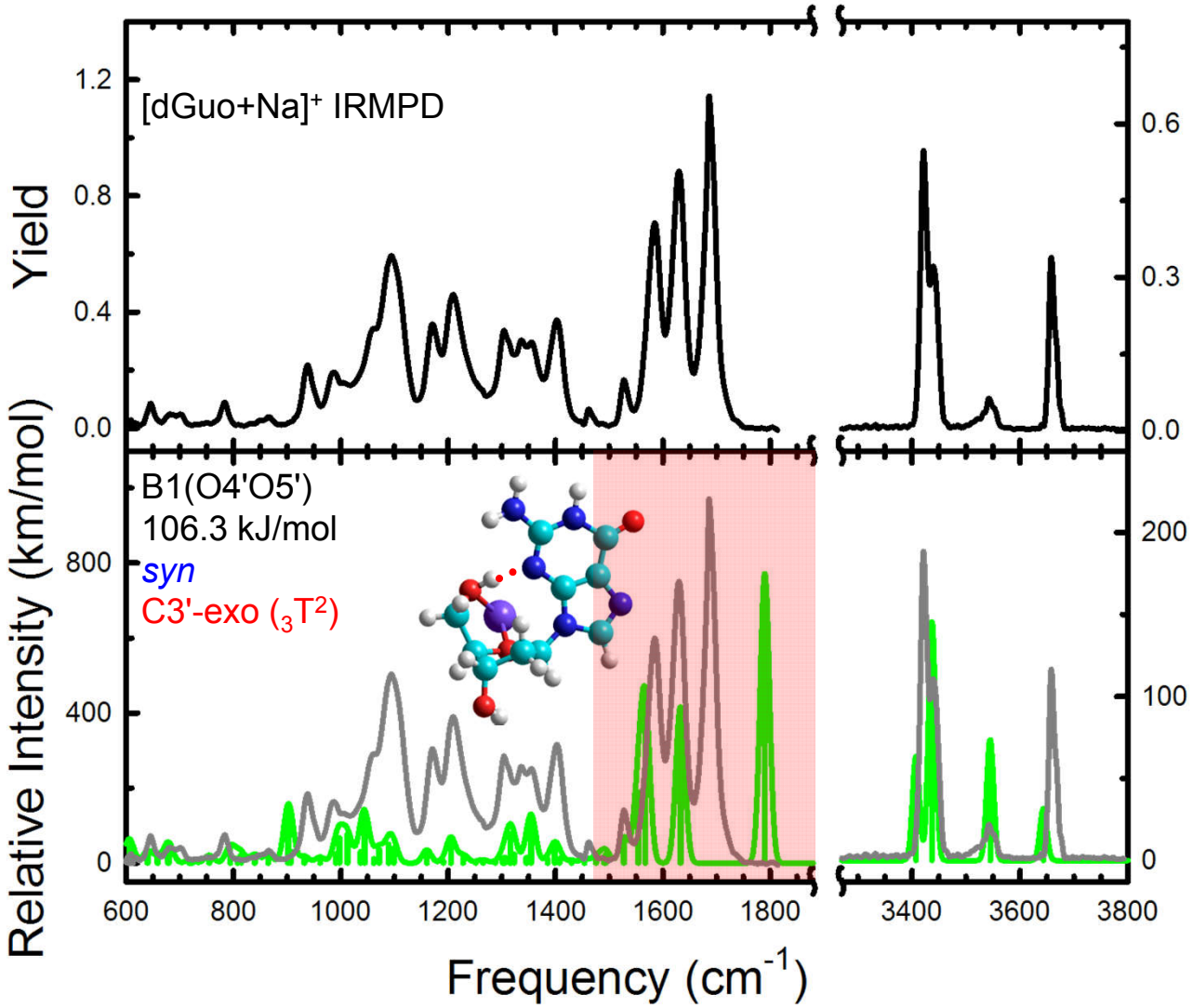
[dGuo+Na]+ IRMPD
Yield
1.2
0.8
0.4
0.0
0.6
0.3
0.0
B1(O4'O5')
106.3 kJ/mol
syn
C3'-exo (3T2)
Relative Intensity (km/mol)
800
400
0
200
100
0
600
800
1000
1200
1400
1600
1800
3400
3600
3800
Frequency (cm-1)

Figure S8.

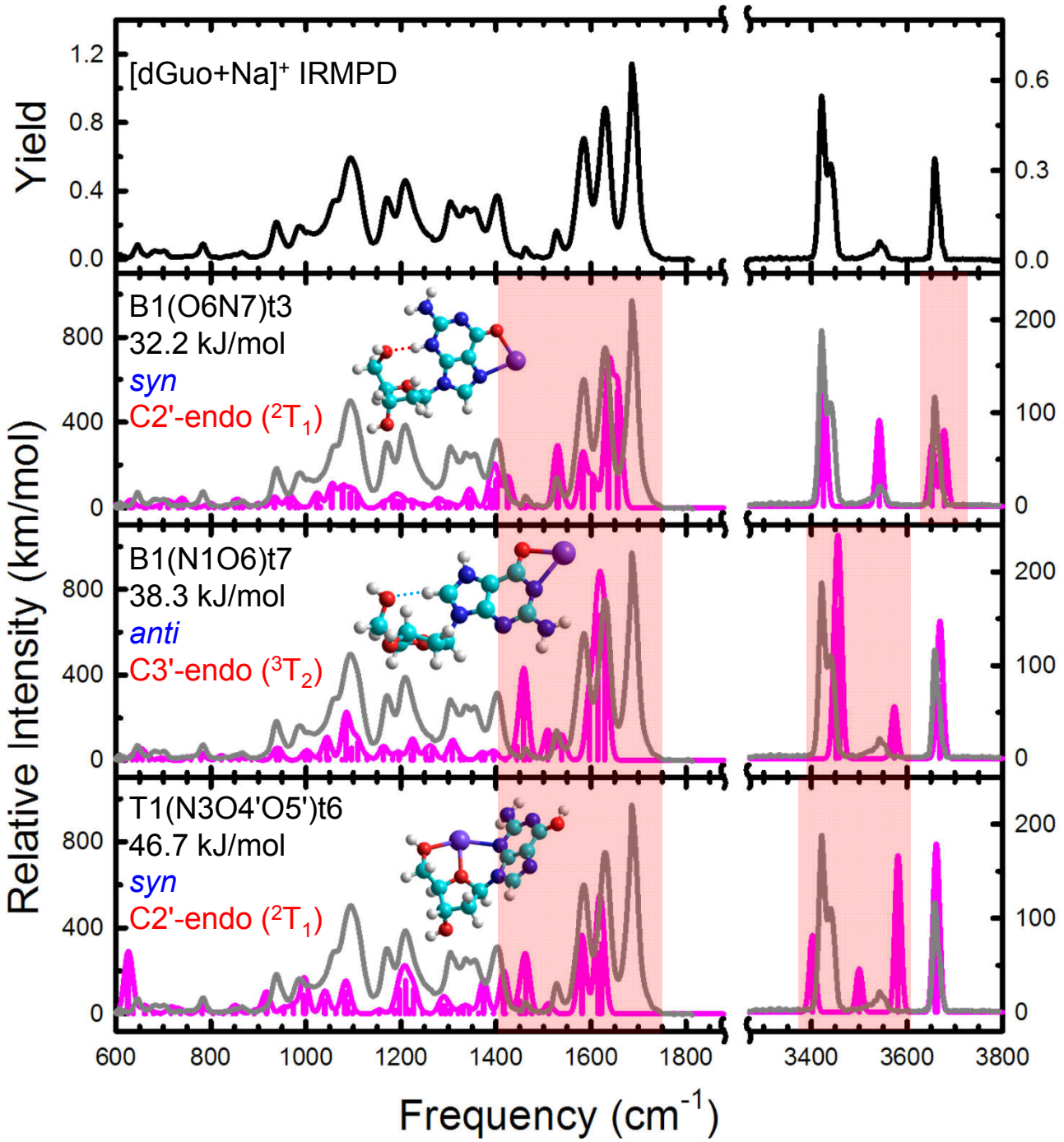
[dGuo+Na]+ IRMPD
Yield
1.2
0.8
0.4
0.0
0.6
0.3
0.0
B1(O6N7)t3
32.2 kJ/mol
syn
C2'-endo (2T1)
B1(N1O6)t7
38.3 kJ/mol
anti
C3'-endo (3T2)
T1(N3O4'O5')t6
46.7 kJ/mol
syn
C2'-endo (2T1)
Relative Intensity (km/mol)
800
400
0
200
100
0
600
800
1000
1200
1400
1600
1800
3400
3600
3800
Frequency (cm-1)

Figure S8.

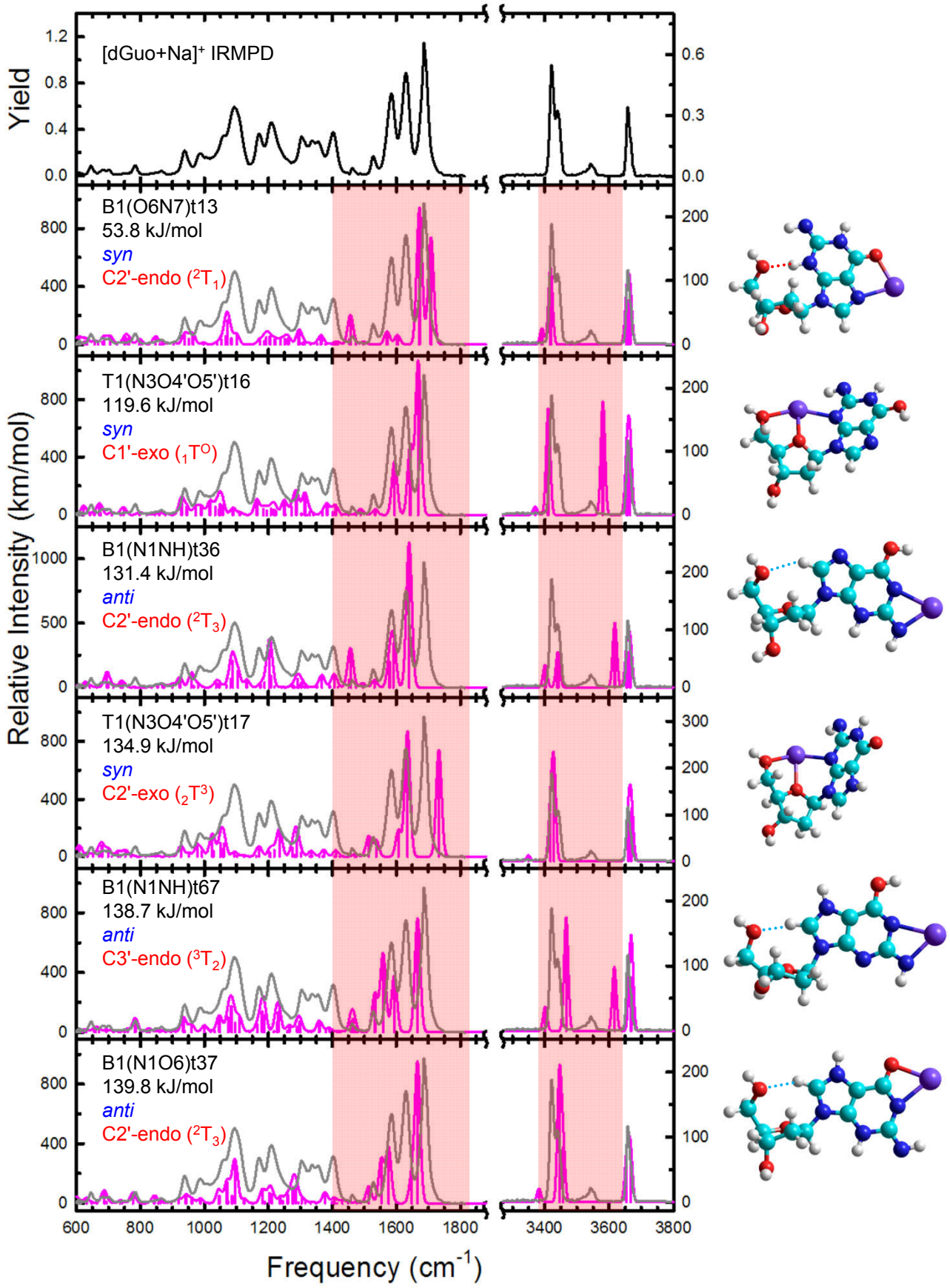
[dGuo+Na]+ IRMPD
Yield
B1(O6N7)t13
53.8 kJ/mol
syn
C2'-endo (2T1)
T1(N3O4'O5')t16
119.6 kJ/mol
syn
C1'-exo (1TO)
B1(N1NH)t36
131.4 kJ/mol
anti
C2'-endo (2T3)
T1(N3O4'O5')t17
134.9 kJ/mol
syn
C2'-exo (2T3)
B1(N1NH)t67
138.7 kJ/mol
anti
C3'-endo (3T2)
B1(N1O6)t37
139.8 kJ/mol
anti
C2'-endo (2T3)
Relative Intensity (km/mol)
Frequency (cm-1)

Figure S9.

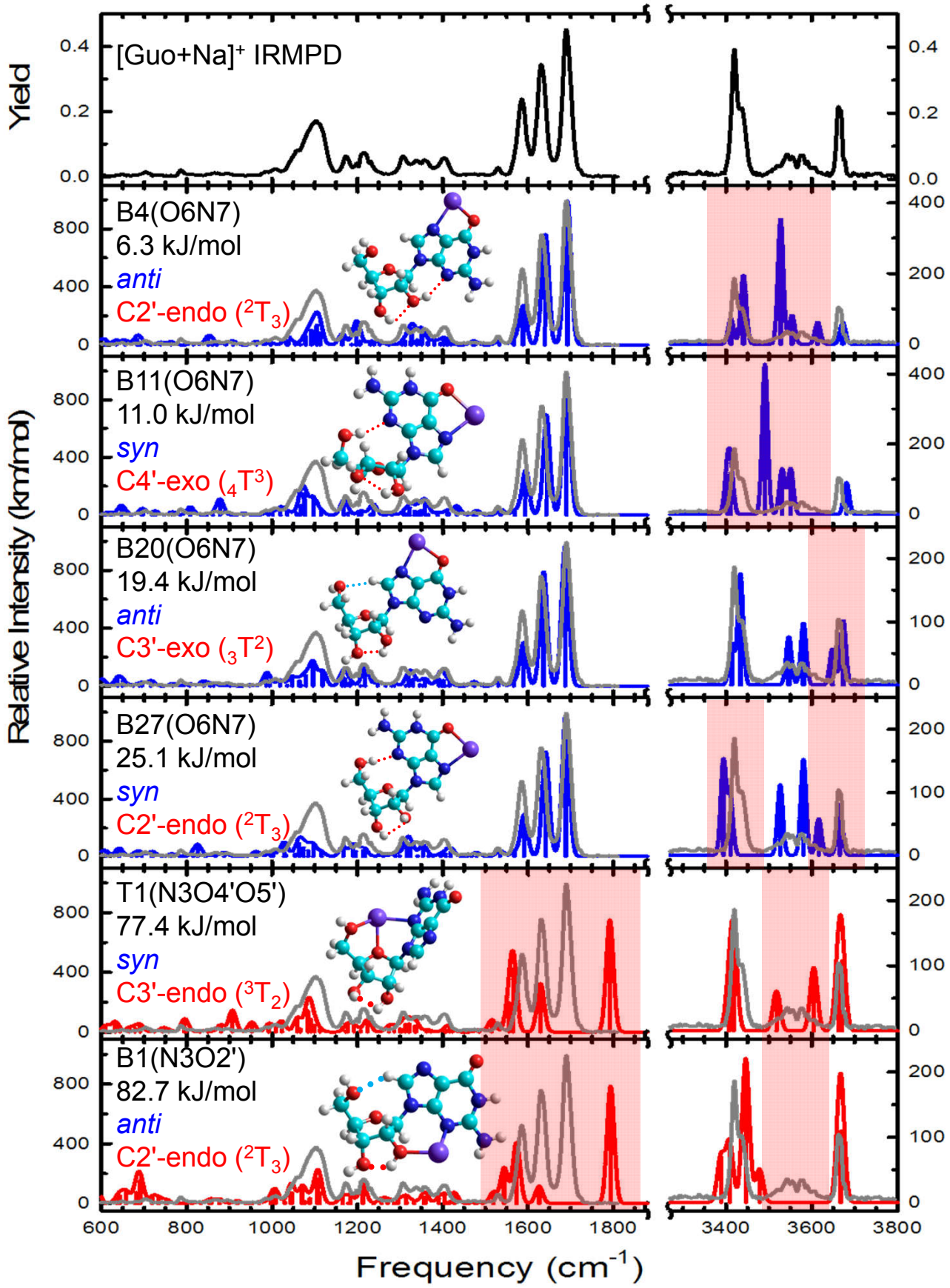
[Guo+Na]+ IRMPD
Yield
B4(O6N7)
6.3 kJ/mol
anti
C2'-endo (2T3)
B11(O6N7)
11.0 kJ/mol
syn
C4'-exo (4T3)
B20(O6N7)
19.4 kJ/mol
anti
C3'-exo (3T2)
B27(O6N7)
25.1 kJ/mol
syn
C2'-endo (2T3)
T1(N3O4'O5')
77.4 kJ/mol
syn
C3'-endo (3T2)
B1(N3O2')
82.7 kJ/mol
anti
C2'-endo (2T3)
Relative Intensity (km/mol)
Frequency (cm-1)

Figure S10.

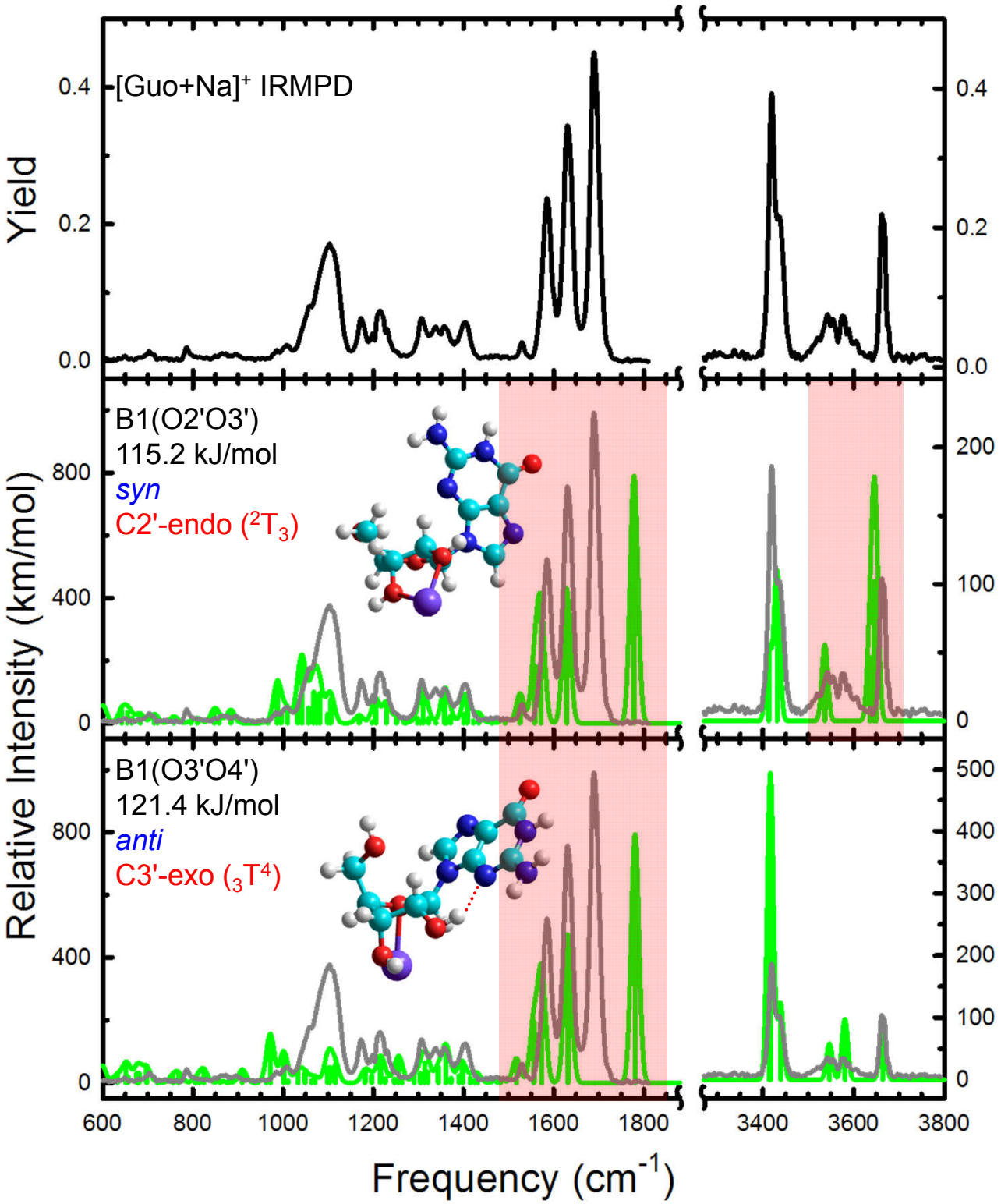
[Guo+Na]+ IRMPD
Yield
0.4
0.2
0.0
B1(O2'O3')
115.2 kJ/mol
syn
C2'-endo (2T3)
B1(O3'O4')
121.4 kJ/mol
anti
C3'-exo (3T4)
Relative Intensity (km/mol)
800
400
0
200
100
500
300
600
1000
1200
1400
1600
1800
3400
3600
3800
Frequency (cm-1)

Figure S11.

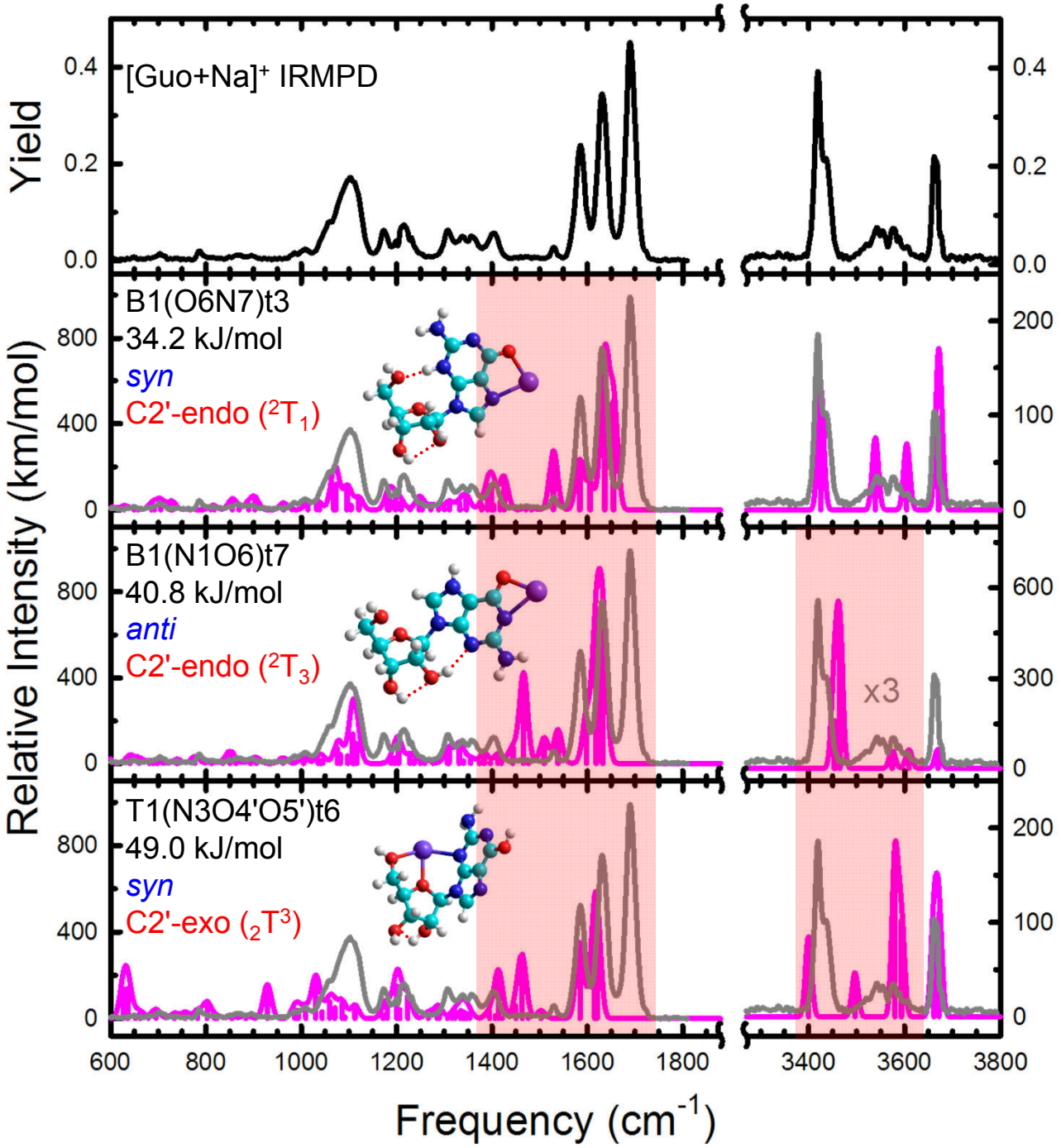
[Guo+Na]+ IRMPD
Yield
0.4
0.2
0.0
B1(O6N7)t3
34.2 kJ/mol
syn
C2'-endo (2T1)
B1(N1O6)t7
40.8 kJ/mol
anti
C2'-endo (2T3)
x3
T1(N3O4'O5')t6
49.0 kJ/mol
syn
C2'-exo (2T3)
Relative Intensity (km/mol)
800
400
0
600
300
200
100
600
800
1000
1200
1400
1600
1800
3400
3600
3800
Frequency (cm-1)

Figure S11.

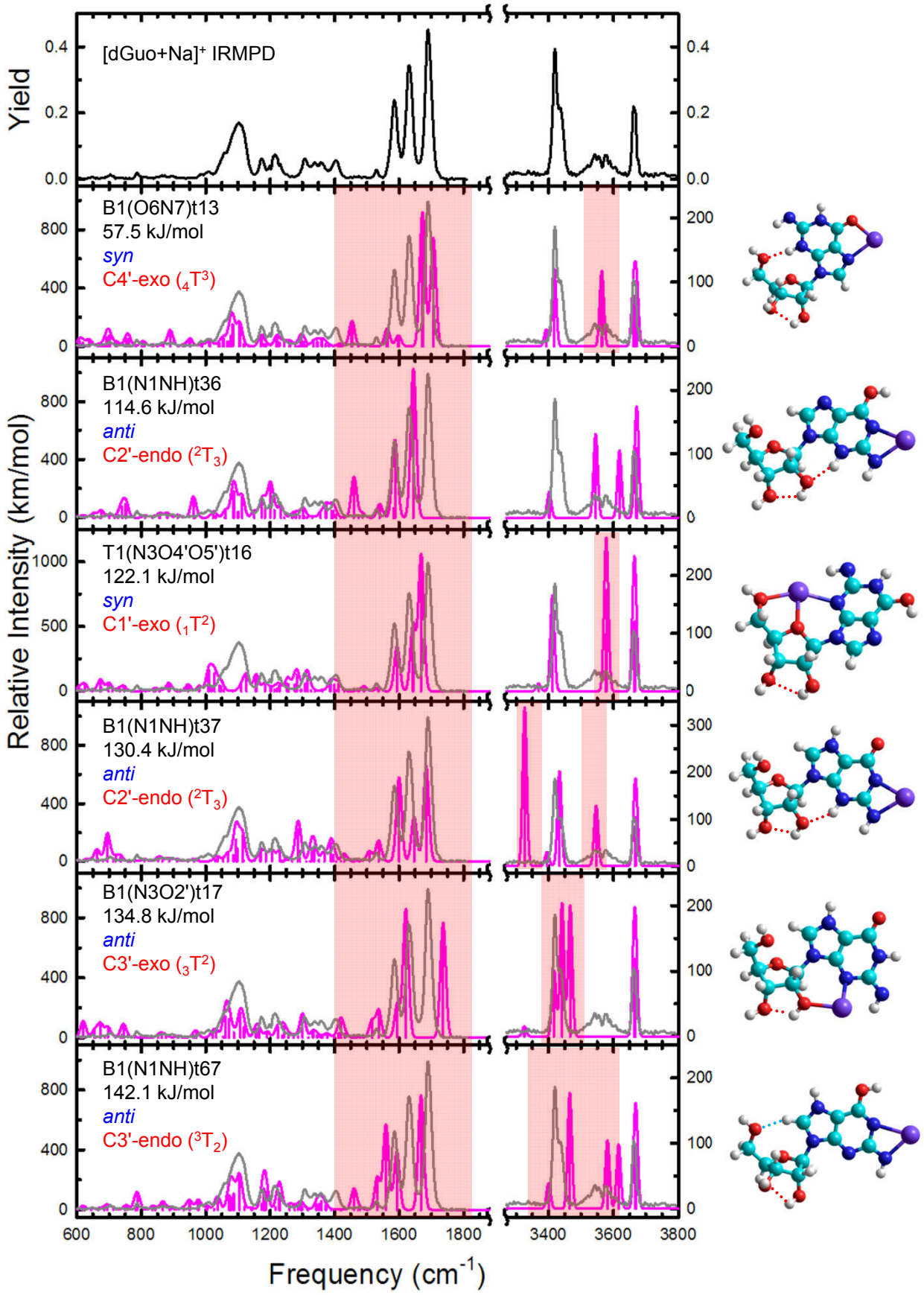
[dGuo+Na]+ IRMPD
Yield
B1(O6N7)t13
57.5 kJ/mol
syn
C4'-exo (4T3)
B1(N1NH)t36
114.6 kJ/mol
anti
C2'-endo (2T3)
T1(N3O4'O5')t16
122.1 kJ/mol
syn
C1'-exo (1T2)
B1(N1NH)t37
130.4 kJ/mol
anti
C2'-endo (2T3)
B1(N3O2')t17
134.8 kJ/mol
anti
C3'-exo (3T2)
B1(N1NH)t67
142.1 kJ/mol
anti
C3'-endo (3T2)
Relative Intensity (km/mol)
Frequency (cm-1)